Mode sensitivity analysis of vertically arranged double hybrid plasmonic waveguide

M. A. BUTT[a,*], N. L. KAZANSKIY[a,b]
[a]*Department of Technical Cybernetic, Samara National Research University, 34 Moskovkoye Shosse, Samara 443086, Russia*
[b]*IPSI RAS-Branch of the FSRC "Crystallography and Photonics" RAS, 151 Molodogvardeiskaya, Samara 443001, Russia*

Herein, we present a numerical investigation of mode sensitivity of a vertically arranged double hybrid plasmonic waveguide structure based on the silicon-on-insulator platform. The waveguide geometry is composed of a silicon core separated by nanogaps from a metal film on both sides. The study is conducted via a 3D finite element method utilizing a commercially available COMSOL software. The width of the silicon core (W_{core}) plays an important role in the formation of a pure strong hybrid mode in the low index medium nanogaps. The device height is fixed at 220 nm whereas the W_{core} is optimized to boost the confinement factor and evanescent field ratio which in turn results in enhanced sensitivity of the hybrid mode. The maximum confinement factor, evanescent field ratio and mode sensitivity of TE polarized hybrid mode are 0.575, 0.695 and 0.938 are obtained at W_{core}=220 nm and g=50 nm, respectively. We believe that our study provides a strategy for the formation of sensitive waveguide structures to be utilized in sensing applications.

(Received June 12, 2020; accepted October 21, 2020)

Keywords: Hybrid plasmonic waveguide, Mode sensitivity, Finite element method, Evanescent field ratio

1. Introduction

Surface plasmons (SPs) are hybrid surface waves produced from the coupling of an electromagnetic wave and free electrons in a metal [1]. It has drawn great concern in recent years because of its extraordinary properties and enormous potential for various functional applications [2-4]. It is believed that SPs provide sub-diffraction- limited confinement of light that is impossible to be achieved by any other means [5-8] and engineer highly integrated optical components and circuits. However, it is shown that light can be confined below the diffraction limit by using an anisotropic material [9]. In terms of the strengths and shortcomings, plasmonic and dielectric waveguides (WGs) complement in certain aspects. Dielectric WG is capable of guiding the light in a high index core based on the principle of total internal reflection. These WGs provide strong mode confinement and usually lossless, however, the mode size is limited by diffraction. Plasmonic WGs on the other hand, can push light well below the diffraction limit but at the expense of a momentous propagation loss. However, there are several plasmonic sensors based on metal-insulator-metal plasmonic WG are recently been proposed which provides quite high sensitivity [10-13].

The hybrid plasmonic waveguide (HPWG) operating mechanism can be represented with the help of the mode-coupling theory. The silicon WG supports dielectric mode while the metal surface supports SPs that are confined near the metal surface. When these two structures are kept together separated by a low index medium. The dielectric WG mode supported by the silicon WG couples to the surface mode supported by the metal [14]. Due to this mode coupling, the light is well confined in the low index region between silicon WG and the metal layer. The hybrid mode is robustly confined than the SP mode, so the HPWG will provide a stronger balance between loss and confinement than the pure plasmonic mode. HPWG provides large light confinement at a lower loss compared with other plasmonic WGs previously reported [14]. Several applications based on hybrid plasmonic WG are recently reported such as sensors [15-17], filters [18], modulators [19], among others. Theoretical studies have shown that a low index layer can retain a low loss compact mode whose propagation length strongly depends on its thickness [7].

2. WG design and numerical simulations

In this work, we presented a mode sensitivity (S_{mode}) analysis of a vertically arranged double hybrid plasmonic waveguide (HPWG) based on SOI platform. Standard HPWG structure consists of a thin layer of low index material sandwiched between the metal layer and a high index dielectric layer. However, our proposed WG geometry is comprised of a silicon core separated by nanogaps (*NGs*) from a metal film on both sides. Gold (*Au*)

is selected as a metal due to its biocompatibility and resistant to oxidation. The height and width of the silicon core are represented as H_{core} and W_{core}, respectively. Whereas the *NGs* is denoted as g which is symmetric on both sides of the silicon core. The device height (H_{core}) is maintained at 220 nm throughout the paper. The proposed WG design is optimized for the TE polarized light at 1550 nm. The schematic of the vertical double HPWG is shown in Fig. 1.

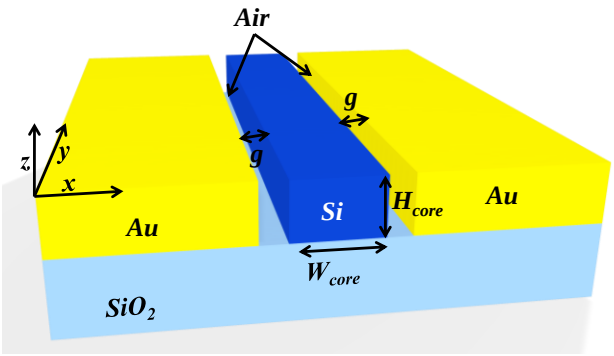

Fig. 1. Schematic of double HPWG (color online)

The numerical investigation is carried out utilizing a commercially available finite element method (FEM) simulation tool (COMSOL Multiphysics 5.1). The x-oriented plane wave is coupled at the input of the WG and the output is collected by the surface integration of the output port. In COMSOL simulations, the dual HPWG design is divided into triangular mesh element with λ/5 grid size, which provides accurate simulation results within the available computational resources. A computational domain with open boundaries is modelled that allows the electromagnetic wave to pass without reflection. An open geometry is approximated by placing a scattering boundary conditions (SBC) at the outer edges of the FEM simulation window. An electric domain is used to launch an x-oriented light into the WG core.

3. Evaluation of confinement factor and evanescent field ratio of double HPWG structure

Silicon photonics has turned out to be very interesting due to its fabrication compatibility with the regular CMOS microelectronics technology [20-22]. For that reason, it is exciting to realize a silicon-based HPWG with basic fabrication processes. For sensing applications, high light-matter interaction is required [23]. Here, we have optimized the WG geometry so that most of the mode power resides in *NGs* which will contribute to the high evanescent field ratio (*EFR*) as a result its sensing capability will be enhanced. The confinement factor (Γ) is the ratio of the intensity integration in the *NG* and overall intensity integration of the WG. As our proposed WG structure has two *NGs*, therefore Γ can be calculated as:

$$\Gamma = \frac{\iiint_{NG1} |E(x,y,z)|^2 dxdydz + \iiint_{NG2} |E(x,y,z)|^2 dxdydz}{\iiint_{total} |E(x,y,z)|^2 dxdydz}$$

The device height is fixed at 220 nm whereas the remaining parameters such as W_{core} and g is varied to find the maximum Γ. W_{core} has varied between 150 nm to 400 nm whereas g is selected in the range of 50 nm to 90 nm. From Fig. 2a, it can be seen that Γ decreases as W_{core} increases due to the formation of dielectric mode in the silicon core. As a result, the power is divided between the hybrid mode and the dielectric mode. For that reason, an optimized value of W_{core} should be selected which allows the formation of strong hybrid mode in the *NGs*. The mode power is also dependent on g. When the separation between metal and high index dielectric material is small, the intensity of the hybrid mode is significantly enhanced. At W_{core}=220 nm and g= 50 nm, the maximum Γ=0.575 is obtained when decreases as W_{core} and g increases. Keeping in mind, the fabrication intolerance of ~20 nm in the value of g, then Γ can fall to 0.511 which is still a decent value.

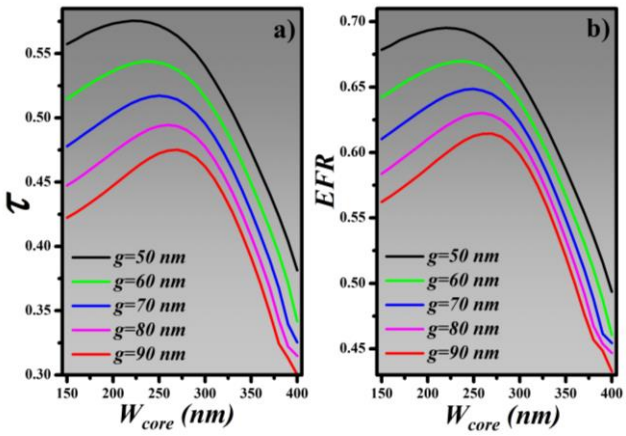

Fig. 2. a) Γ, b) EFR, evaluation of double HPWG. H_{core} is maintained at 220 nm (color online)

Subsequently, the evanescent field ratio (*EFR*) of the vertically arranged double HPWG is considered. An evanescent field is an oscillating electric/magnetic field that does not propagate in a WG core as an electromagnetic wave but whose energy is spatially strong in the cladding region. Every gas has a distinctive absorption peak and is known as a fingerprint for that particular gas. Once the WG sensor is exposed to a gaseous medium, the evanescent field interacts with that gas resulting in a power decay of the transmitting mode if it correlates with the absorption line of the measurand gas. The *EFR* of our proposed WG structure is calculated by taking the ratio of the intensity integration in the nanogaps

(*NGs*) + upper cladding (*UC*) and the overall intensity integration of the WG structure which can be expressed as:

$$EFR = \frac{\iiint_{NGs+UC} |E(x,y,z)|^2 dxdydz}{\iiint_{total} |E(x,y,z)|^2 dxdydz}$$

The *EFR* of TE hybrid mode mainly depends on Γ. Stronger Γ leads to high *EFR* as shown in Fig. 2b. The best *EFR*=0.695 is obtained for W_{core}=220 nm and g= 50 nm. This value is significantly higher than the *EFR* offered by most of the standard WG structures such as rib and ridge [24, 25].

To validate the point, the E-field distribution in the double HPWG is represented in the top view and cross-section view. Fig. 3a presents the E-field distribution in the WG is taken along *xy*-plane at H_{core}/2. The 3D representation of the hybrid mode in the double HPWG is displayed in Fig. 3b which shows the symmetric mode power distribution in the *NGs*. Whereas the cross-section view is taken along *xz*-plane in the middle of the WG as depicted in Fig. 2(c,d,e). It can be seen that at W_{core}=220 nm, the WG geometry is not capable of supporting a dielectric mode in the silicon core. As a result, almost all mode power is transformed into a hybrid mode. As W_{core} > 300 nm, the dielectric mode is formed in the core resulting in a power division between core and *NGs*.

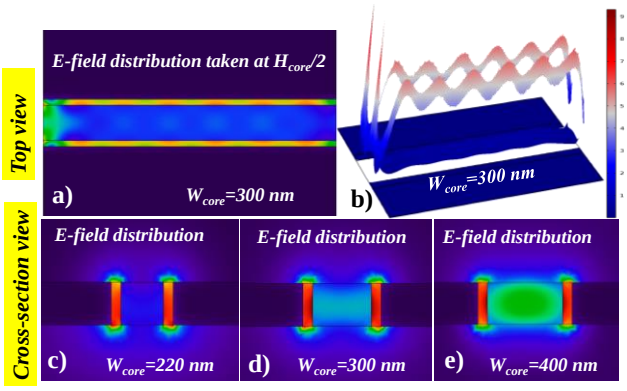

Fig. 3. E-field distribution in the double HPWG a) Top view taken along xy-plane at H_{core}/2, b) 3D representation of E-field in the WG. Cross-section view taken along xz-plane c) W_{core}=220 nm, d) W_{core}=300 nm, e) W_{core}=400 nm (color online)

4. Evaluation of effective refractive index and mode sensitivity of double HPWG structure

For sensing applications, the mode sensitivity (S_{mode}) is a critical parameter which should be taken into consideration while designing the optical WGs [26]. S_{mode} is evaluated by using the following formula:

$$S_{mode} = \frac{n_{eff2} - n_{eff1}}{n_2 - n_1},$$

Where n_{eff2} is the effective refractive index at the refractive index of the analyte (n_2) and n_{eff1} is the effective refractive index at the refractive index of air (n_1). In this analysis, n_2=1.35 is considered to calculate the sensitivity of TE hybrid mode. The real part of n_{eff} is calculated concerning W_{core} and g as shown in Fig. 4a. At optimized WG geometry, a significant portion of the optical field is located within the low-index *NGs*, that's why the n_{eff} of the double HPWG is significantly lower than the high index core standard WGs. However, an increase in the W_{core} of the WG leads to an increase in n_{eff} (~2.25) due to the formation of dielectric mode in the high index core. It is believed that if W_{core} is large enough to support a pure dielectric mode then n_{eff} can even become higher than 3.

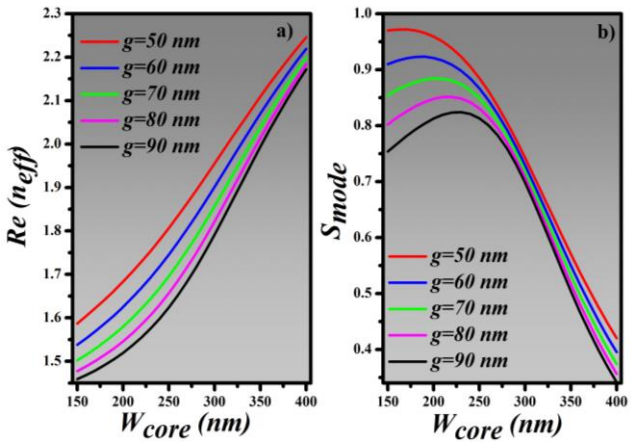

Fig. 4. a) Real part of the effective refractive index of the WG, b) Mode sensitivity of the WG. H_{core} is maintained at 220 nm (color online)

The S_{mode} of vertically arranged double HPWG is calculated concerning W_{core} and g as shown in Fig. 4b. The S_{mode}> 90% can be obtained by enhancing the *EFR* of the hybrid mode. At W_{core}=220 nm and g=50 nm, S_{mode}=0.938 is obtained which makes this WG highly responsive to the ambient refractive index. As a result, a small change in refractive index can be sensed by these WG structures. However, optical losses are directly related to the waveguide parameters. As the waveguide dimensions reduces, it offers a high S_{mode} at the cost of high propagation loss as demonstrated in our previous paper [27]. Keeping in mind the available laser power, the waveguide dimensions should be designed to have an optimum S_{mode} and losses.

The fabrication of the proposed WG structure can be realized on a standard SOI platform via standard CMOS technology. The WG core is formed by dry or wet etching the unwanted *Si* layer followed by a deposition of *Au* layer of same height on both sides of a core by keeping a small gap between *Si* and *Au*.

5. Conclusion

In conclusion, we presented a mode sensitivity analysis

of a vertically configured double hybrid plasmonic waveguide structure based on SOI platform. The waveguide geometry is quite attractive which provides a strong TE polarized hybrid mode confinement in the low index nanogaps positioned between gold and the silicon layers. The study is conducted via a 3D finite element method. By optimizing the waveguide geometry, the confinement factor of ~0.575 can be obtained at W_{core}= 220 nm and g=50 nm. The mode confinement is directly related to the evanescent field ratio which is a critical parameter defining the light-matter interaction. At an optimized waveguide geometry, a high evanescent field ratio of ~0.695 is obtained which ensures the strong light-matter interaction. When the biggest portion of the mode is directly exposed to the surrounding medium, a small change in ambient refractive index can bring a big shift in the effective refractive index of the propagating mode. Consequently, the sensitivity of the hybrid mode propagating in the dual hybrid plasmonic waveguide is enhanced. The calculated mode sensitivity of 0.938 can be obtained by maintaining W_{core} and g at 220 nm and 50 nm, respectively.

Acknowledgements

This work was financially supported by the Ministry of Science and Higher Education within the State assignment FSRC «Crystallography and Photonics» RAS (No. 007-GZ/Ch3363/26) for numerical calculations and Russian Science Foundation (No 20-69-47110) for theoretical results.

References

[1] A. R. Zakharian, J. V. Moloney, M. Mansuripur, Optics Express **15**, 183 (2007).
[2] S. A. Maier, A Plasmonics: Fundamentals and Applications (Springer) (2007).
[3] N. L. Kazanskiy, S. N. Khonina, M. A. Butt, Physica E **117**, 113798 (2020).
[4] N. L. Kazanskiy, M. A. Butt, Phot. Lett. Poland **12**, 1 (2020).
[5] D. K. Gramotnev, S. I. Bozhevolnyi, Nature Photonics **4**, 83 (2010).
[6] M. A. Butt, N. L. Kazanskiy, S. N. Khonina, Photonic Sensors **10**, 223 (2020).
[7] M. A. Butt, N. L. Kazanskiy, S. N. Khonina, Laser Physics **30**, 076204 (2020).
[8] M. A. Butt, S. A. Fomchenkov, Proc. SPIE **11516**, Optical Technologies for Telecommunications 115160G-1 (2020).
[9] S. Jahani, Z. Jacob, Optica **1**, 96 (2014).
[10] J. Lee, J. Song, G. Y. Sung, J. H. Shin, Nano Lett. **14**, 5533 (2014).
[11] K. V. Voronin, Y. V. Stebunov, A. A. Voronov, A. V. Arsenin, V. S. Volkov, Sensors **20**, 203 (2020).
[12] N. L. Kazanskiy, M. A. Butt, S. N. Khonina, Photonics and Nanostructures-Fundamentals and Applications 42, 100836 (2020).
[13] X-Y. Zhang, A. Hu, J. Z. Wen, T. Zhang, X-J. Xue, Y. Zhou, W. W. Duley, Optics Express **18**, 18945 (2010).
[14] M. A. Butt, N. L. Kazanskiy, S. N. Khonina, Laser Physics **30**, 016202 (2020).
[15] L. Zhou, X. Sun, X. Li, J. Chen, Sensors **11**, 6856 (2011).
[16] J. Guo et al., Light: Science & Applications **9**, 29 (2020).
[17] M. A. Butt, S. N. Khonina, N. L. Kazanskiy, Journal of Modern Optics **65**, 1135 (2018).
[18] M. Z. Alam, F. Bahrami, J. S. Aitchison, M. Mojahedi, IEEE Photonics Journal **6**, 3700110 (2014).
[19] D. Ansell, I. P. Radko, Z. Han, F. J. Rodriguez, S. I. Bozhevolnyi, A. N. Grigorenko, Nature Communications **6**, 8846 (2015).
[20] R. F. Oulton, V. J. Sorger, D. A. Genov, D. F. P. Pile, X. Zhang, Nature Photonics **2**, 496 (2008).
[21] M. A. Butt, S. N. Khonina, N. L. Kazanskiy, Computer Optics **43**, 1079 (2019).
[22] P. P. Absil, P. Verheyen, P. D. Heyn, M. Pantouvaki, G. Lepage, J. D. Coster, J. V. Campenhout, Optics Express **23**, 9369 (2015).
[23] M. A. Butt, S. N. Khonina, N. L. Kazanskiy, Waves in Random and Complex Media **30**, 292 (2020).
[24] M. A. Butt, S. N. Khonina, N. L. Kazanskiy, Optik **168,** 692 (2018).
[25] M. A. Butt, S. A. Degtyarev, S. N. Khonina, N. L. Kazanskiy, Journal of Modern Optics **64**, 1892 (2017).
[26] M. Odeh, K. Twayana, K. Sloyan, J. E. Villegas, S. Chandran, M. S. Dahlem, IEEE Photonics Journal **11**, 2700210 (2019).
[27] M. A. Butt, N. L. Kazanskiy, S. N. Khonina, IEEE Sensors Journal **20**, 9779 (2020).

*Corresponding author: ali_ciit_engineer@yahoo.com